agriculture

MDPI

Article

Genome-Wide Characterization of the Common Buckwheat B-Box Gene Family and Identification of FeBBX11 and FeBBX27 Involved in Flavonoid Biosynthesis

Leyun Li [1], Yuting Li [1], Yingjie Bian [1], Zhixiong Liu [2], Zehao Hou [1,*] and Zhengwu Fang [1]

[1] MARA Key Laboratory of Sustainable Crop Production in the Middle Reaches of the Yangtze River (Co-Construction by Ministry and Province), Hubei Key Laboratory of Waterlogging Disaster and Agricultural Use of Wetland, College of Agriculture, Yangtze University, Jingzhou 434025, China; 18748980234@163.com (L.L.); liyt@yangtzeu.edu.cn (Y.L.); 15733223963@163.com (Y.B.); fangzhengwu88@163.com (Z.F.)

[2] College of Horticulture and Gardening, Yangtze University, Jingzhou 434000, China; zxliu77@yahoo.com

* Correspondence: houzh@yangtzeu.edu.cn

Abstract

Flavonoids, a class of secondary metabolites in higher plants, exert a broad range of health-promoting effects by enhancing antioxidant activity. B-box (BBX) transcription factors are reportedly involved in the regulation of flavonoid biosynthesis. However, the roles and functions of common buckwheat (*Fagopyrum esculentum* Moench)'s BBX members in flavonoid biosynthesis remain unclear. In this study, 31 FeBBX members were identified and divided into five subgroups. Multiple *cis*-elements responsive to light, hormone, and stress signals were found in the promoter regions of these members, and transcriptome data showed two different expression patterns of FeBBX11 and FeBBX27 induced by light. Subcellular location localized *FeBBX11* and *FeBBX27* proteins in the nucleus. The overexpression of *FeBBX11* and *FeBBX27* in common buckwheat enhanced its flavonoid biosynthesis and antioxidant activity. These results provide a foundation for further research on the regulatory role of the *BBX* gene family in flavonoid biosynthesis.

Keywords: flavonoids; the *BBX* gene family; common buckwheat; light

1. Introduction

Flavonoids are some of the most widely distributed and abundant secondary metabolites in higher plants [1]. Their basic skeleton is C6-C3-C6, containing rich double bonds and phenolic hydroxyl groups [2]. Based on their molecular structures, flavonoids are generally classified as either flavones, isoflavones, flavanols, or anthocyanins [3]. Phenylalanine is the initial substrate for plant flavonoid biosynthesis: It is first converted into cinnamic acid and, then, under the action of related enzymes, into 4-coumaroyl CoA. This compound then condenses with malonyl CoA to form chalcone, which is converted into flavanone under the action of chalcone isomerase (CHI). Flavanone then generates various dihydroflavonol intermediates; from these, it enters various downstream branches. In one such branch, flavonols are synthesized under the catalysis of flavonol synthase (FLS) [4]. Flavonoids can regulate oxidative stress levels by reducing malondialdehyde (MDA) content and increasing the activities of antioxidant enzymes such as superoxide dismutase (SOD), thereby alleviating oxidative damage in human tissues [5]. They also play important roles in regulating inflammatory responses, fighting viral infections, and inhibiting ferroptosis [6–8]. The main flavonoid components of buckwheat are rutin, quercetin, kaempferol,

Check for updates

Academic Editor: Rodomiro Ortiz

Received: 27 August 2026
Revised: 5 October 2026
Accepted: 6 October 2026
Published: 9 October 2026

Copyright: © 2026 by the authors. Licensee MDPI, Basel, Switzerland. This article is an open access article distributed under the terms and conditions of the Creative Commons Attribution (CC BY) license.

and their derivatives; among these, rutin accounts for 50% to 90% of the total flavonoids [9]. The flavonoid content varies not only among buckwheat varieties but also among tissues and organs within the same variety [10]. The seed coat color is associated with flavonoid content; generally, darker seeds contain higher flavonoid levels [11]. Moreover, flavonoid accumulation in buckwheat exhibits tissue specificity and varying spatiotemporal distribution patterns depending on growth stage, and light has been shown to influence its synthesis [12,13].

Flavonoid biosynthesis is jointly regulated by structural enzymes and transcription factors. At the enzymatic level, a series of core enzymes determine the metabolic flux and final yield of flavonoids: phenylalanine ammonia-lyase (PAL), chalcone synthase (CHS), CHI, dihydroflavonol 4-reductase (DFR), flavonoid 3′-hydroxylase (F3′H), flavonoid 3′,5′-hydroxylase (F3′5′H), etc. [14]. These enzymes' expression levels are closely associated with flavonoid accumulation. For example, the overexpression of the *CHS* gene in *Rhododendron delavayi* significantly increased flavonoid content in transgenic lines [15], and similar results were obtained by overexpressing the *CHI* gene in rice [16]. The *PAL* gene in citrus has also been confirmed to participate in regulating lignin and flavonoid biosynthesis [17]. At the transcriptional regulation level, a ternary protein complex—MYB, bHLH, and WD40 proteins—often finely regulates flavonoid metabolism by modulating the expression of structural genes [18]. In *Lonicera japonica*, MYB transcription factors activate *LjaC4L* and *LjaCHS* expression by binding to their promoters, thereby regulating the synthesis of floral flavonoids [19]. In buckwheat, several functional genes have a confirmed association with flavonoid synthesis, including *FtUFGT* [20], *FeF3′H* [21], and *FtC4H* [22]. Moreover, an NAC transcription factor was found to activate *FtF3′H* and *FtF3′5′H* transcription, influencing flavonoid biosynthesis in Tartary buckwheat [23]. Flavonoid biosynthesis is also synergistically affected by environmental factors such as light, inorganic salts, and biological factors [24], with light being a key factor affecting flavonoid metabolism in buckwheat [25]. Enhanced UV-B radiation induces flavonoid accumulation in Tartary buckwheat; this is closely associated with reduced stress damage and improved antioxidant enzyme activity [26].

The B-box (BBX) proteins are a subfamily of zinc finger transcription factors. They contain B-box domains at the N-terminus, and some members also possess a CCT domain at the C-terminus [27]. BBX proteins were first identified as central regulators of flowering time through their modulation of the floral integrator gene FT [28]. Beyond their roles in flowering, BBX proteins also participate in plants' secondary metabolism [29]. BBX transcription factors mediate light signaling and have recently been shown to regulate flavonoid biosynthesis. In *Populus tremula*, PtrBBX20 activates the transcription of proanthocyanidin- and anthocyanin-specific genes under light conditions and functions alongside PtrHY5 to promote anthocyanin accumulation [30]. An IbBBX transcriptional cascade finely regulates anthocyanin accumulation in the leaves of *Ipomoea batatas* [31]. *MdBBX47* in *Malus domestica Borkh* has also been identified as a key gene controlling anthocyanin accumulation [32]. The expression of *BBX* genes exhibits spatiotemporal specificity. For example, *Vaccinium corymbosum VcBBX* genes are highly expressed during flower bud differentiation, full-bloom, and petal-fall stages [33]. *MsBBX41/44/48/54* genes are predominantly expressed in the floral organs of *Medicago sativa*, suggesting their involvement in flower development and metabolic regulation [34]. Despite the increasing amount of evidence suggesting BBX functions in other plant species, reports are lacking regarding the family characteristics and regulatory roles of BBX members in common buckwheat (*Fagopyrum esculentum*). In this study, we identified 31 *FeBBX* genes from the common buckwheat genome database and performed a comprehensive family analysis. Using flavonoid synthesis data and bioinformatics screening, we identified two key BBX proteins: FeBBX11 and FeBBX27 act

as positive regulators promoting flavonoid accumulation. This study expands the current understanding of the BBX transcription factor family in common buckwheat, and the key members identified herein may be targeted in future breeding of buckwheat varieties with enhanced flavonoid content.

2. Materials and Methods

2.1. Identification of FeBBX Proteins

We identified the B-box domain across the buckwheat genome in order to detect FeBBX proteins using a Hidden Markov Model (HMM) profile of the B-box domain (Pfam accession PF00643), with an E-value threshold of 1×10^{-5}. We used the chromosome-level assembly pintian for the common buckwheat genome (Fagopyrum esculentum pintian, http://47.93.16.146/home#/download, accessed on 9 August 2025). The numbers of B-box and CCT domains in the *FeBBX* genes were further verified using the NCBI CD-Search tool. We removed redundant sequences with 100% identity and considered only the longest transcript per locus. Consequently, we used the TBtools software (v2.554) to analyze the physicochemical characteristics of the FeBBX proteins, including the number of amino acids, the molecular weight, and other physicochemical coefficients [35]. Subcellular localization was predicted using the online tool Cell-PLoc 2.0, specifically the Plant-mPLoc predictor (http://www.csbio.sjtu.edu.cn/bioinf/plant-multi/, accessed on 9 September 2025).

2.2. Phylogenetic Tree, Gene Structures, Conserved Domains and Motif Analysis

The protein sequences of 32 AtBBX family genes were downloaded from the Arabidopsis Information Resource (TAIR), while the genomic and coding sequences of each FeBBX gene were retrieved from BuckwheatGPDB. We performed multiple sequence alignment of the BBX protein sequences using the ClustalW algorithm implemented in MEGA 11.0 with default parameters (Gonnet substitution matrix, gap opening penalty = 10, gap extension penalty = 0.2) [36]. Poorly aligned regions and gaps were treated using the partial deletion option with a site coverage cutoff of 95%. Phylogenetic trees were constructed using the maximum-likelihood (ML) method with the best-fitting substitution model LG + F + I + G4, selected using the Find Best Protein Models (ML) tool according to the Bayesian Information Criterion (BIC). Node support was assessed with 1000 bootstrap replicates. The initial tree(s) for the heuristic search were obtained automatically by applying Neighbor-Joining to a matrix of p-distances estimated using the LG model. For synteny analysis, the One-Step MCScanX function implemented in TBtools was used to identify both intra-genomic and inter-species collinear gene pairs between common buckwheat and Arabidopsis. The analysis was performed with default parameters (an E-value threshold of 1×10^{-10} and a maximum of 5 BLAST hits per query). The gene structures and consensus sequences for the B-box and CCT domains of 31 FeBBXs were visualized using TBtools [37].

2.3. Promoter Analysis

We extracted the 2500 bp promoter sequences upstream of the translation start site (ATG) of each *FeBBX* gene from the common buckwheat genome using the Gtf/Gff3SequenceExtract tool implemented in the TBtools software [37]. The extracted sequences were submitted to the PlantCARE database (http://bioinformatics.psb.ugent.be/webtools/plantcare/html/, accessed on 9 September 2025) to identify cis-acting regulatory elements using default parameters. These were manually curated and categorized by function (e.g., hormone-responsive, stress-responsive, or light-responsive).

2.4. Subcellular Localization

To perform the subcellular localization of the FeBBX proteins, the whole-length coding sequences of *FeBBX11* and *FeBBX27* were cloned into the pHZM27g-GFP vector under the control of the 2 × CaMV35S promoter to generate the pHZM27g-GFP-FeBBX11/27 fusion proteins in October 2025. The recombinant vectors were introduced into *Agrobacterium tumefaciens* strain GV3101, and the Green Fluorescent Protein (GFP) was visualized and imaged using a confocal microscope (Leica, Wetzlar, Germany) in December 2025 [38]. The Agrobacterium cultures harboring the fusion constructs were resuspended in infiltration buffer (10 mM MES, 10 mM $MgCl_2$, and 200 μM acetosyringone) to an OD_{600} of approximately 0.6. They were then incubated at room temperature for 2–3 h prior to infiltration. The bacterial suspension was infiltrated into the leaves of Nicotiana benthamiana plants using a needleless syringe. The infiltrated plants were maintained in a growth chamber at 22–25 °C under a photoperiod of 16 h light/8 h dark. Leaf samples were examined 2–3 days post-infiltration (dpi).

2.5. Analysis of Expression Pattern Data of FeBBXs

The transcriptome data for this study was downloaded from the China National Center for Bioinformation's GSA database (PRJCA009237 and PRJCA066737). The dataset of PRJCA009237 includes root, stem, leaf, flower, and caryopsis samples of common buckwheat, with three biological replicates per tissue. For the light-responsive expression analysis (PRJCA066737), the common buckwheat cultivar used in this study was 'QZZTQ', a laboratory-bred line. Seedlings were subjected to three treatments of varying light intensity–dark (0 Lux), 400 Lux, and 1000 Lux under a 16 h light/8 h dark photoperiod for two weeks. Cotyledons were harvested as the experimental samples, with three biological replicates per treatment. Gene expression levels were quantified as FPKM values. The FPKM values were transformed using $\log_2$(FPKM + 1) for heatmap visualization. Hierarchical clustering analysis was performed using the TBtools software with default parameters.

2.6. Overexpression of FeBBX11 and FeBBX 27 in Hairy Root

The recombinant vectors pHZM27g-GFP-FeBBX11 and pHZM27g-GFP-FeBBX27, constructed in Section 2.3, were transferred into *Agrobacterium tumefaciens* strain K599 in March 2026. Common buckwheat transformation was performed as previously described to generate hairy root [39]. The common buckwheat (*Fagopyrum esculentum*) cultivar 'QZZTQ' was used for hairy root transformation. Seeds were surface-sterilized and germinated in MS culture flasks, and cotyledons and hypocotyls from 7–10-day-old seedlings were excised as explants. The Agrobacterium K599 was grown to an OD_{600} of 0.6–0.8. The explants were immersed in the bacterial suspension for 2–5 min with gentle shaking. After infection, the explants were blotted dry on sterile filter paper and co-cultivated on MS solid medium at 25 °C in the dark for 2 days. Following co-culture, the explants were transferred to MS solid medium containing 200 mg/L of cefotaxime sodium to eliminate bacteria, and they were cultured at 25 °C until the roots differentiated.

2.7. RNA Extraction, cDNA Synthesis, PCR or qRT-PCR Conditions

Total RNA was extracted from hairy root samples using the RNA Easy Fast Plant Tissue Kit (Tiangen, Beijing, China) according to the manufacturer's instructions. First-strand cDNA was synthesized from [1 μg] of total RNA using the Geno IV First Strand cDNA Synthesis Kit (GenOrigin, Beijing, China) in a total volume of 10 μL, following the manufacturer's protocol. RT-qPCR was performed using 2 × ChamQ Blue Universal SYBR qPCR Master Mix (Vazyme, Nanjing, China). Each reaction mixture contained 10 μL of 2 × ChamQ Blue Universal SYBR qPCR Master Mix, 0.4 μL of each primer (10 μM),

2 μL of diluted cDNA, and 7.2 μL of RNase-free water. The amplification program was as follows: 95 °C for 30 s; 40 cycles of 95 °C for 10 s and 60 °C for 30 s; melting curves were generated from 60 °C to 95 °C to confirm amplification specificity. No-template controls were included for each primer pair. Each sample was run in three technical replicates. The reference gene Fe-actin was used as the internal control, and its stability across samples was confirmed by geNorm analysis. Relative expression levels were calculated using the $2^{-\Delta\Delta Ct}$ method. The primers used for RT-qPCR are listed in Supplementary Table S2, and all primers were designed using SnapGene (v4.1.9) software.

2.8. Determinations of Total Phenolics, Total Flavonoids, and Antioxidant Capacities

The transformed positive hairy roots of buckwheat were collected in April 2026 and washed thoroughly with distilled water. The samples were pulverized into a finer powder under liquid nitrogen. We weighed 0.2 g of each sample and added 10 mL of methanolic HCl (1%). The mixture was shaken at 4 °C in the dark for 24 h, followed by centrifugation at 4000 rpm for 10 min, after which the supernatant fluid was collected. Then, we sucked a 500 μL portion of the supernatant mixed with equal volumes of distilled water and chloroform to eliminate chlorophyll and lipid-soluble impurities. The mixture was then centrifuged at 4 °C and 12,000 rpm for 15 min. The upper aqueous layer was recovered and kept at −20 °C until further analysis.

The total phenolic content was measured using the Folin–Ciocalteu method [40]. The total flavonoid content was determined by the sodium nitrite–aluminum chloride–sodium hydroxide colorimetric method [41]. We determined the FRAP antioxidant capacity and ABTS radical scavenging activity using Trolox as the reference standard [42,43].

2.9. Statistical Analysis

All experiments were performed with three independent biological replicates (n = 3), each with three technical replicates (n = 3). Each biological replicate corresponds to an independent transformation event, an independently generated hairy root line derived from a separate transformation experiment, and each line was individually confirmed by PCR/RT-qPCR to stably overexpress the target gene. Data are presented as mean ± SD. Statistical analyses were performed using SPSS 26.0. Two-group comparisons were performed using a two-tailed unpaired Student's t-test. Multiple-group comparisons among the empty-vector control and the two gene-overexpressing hairy root lines were performed using one-way ANOVA followed by Tukey's post hoc test. different letters denote significant differences.

3. Results

3.1. Identification and Characteristics of FeBBXs

The FeBBX proteins were classified into five subgroups (I–V) based on sequence homology with AtBBX (Figure 1). Detailed information on the FeBBX proteins was predicted and is provided in Table S1. The number of amino acids of the 31 FeBBX proteins ranged from 141 aa (FeBBX30) to 442 aa (FeBBX6), and their molecular weights ranged from 15,927.09 Da (FeBBX30) to 48,159.71 Da (FeBBX6). The isoelectric points ranged from 4.47 (FeBBX17) to 8.55 (FeBBX19). The instability indices of the 31 BBX proteins were above 40, indicating them as unstable proteins. The aliphatic indices ranged from 54.17 (FeBBX10) to 86.32 (FeBBX12). The values of the grand average of hydropathicity were all negative, classifying every FeBBX protein as hydrophilic. Subcellular localization prediction showed that all 31 FeBBX proteins are targeted to the nucleus, suggesting their potential function as transcription factors.

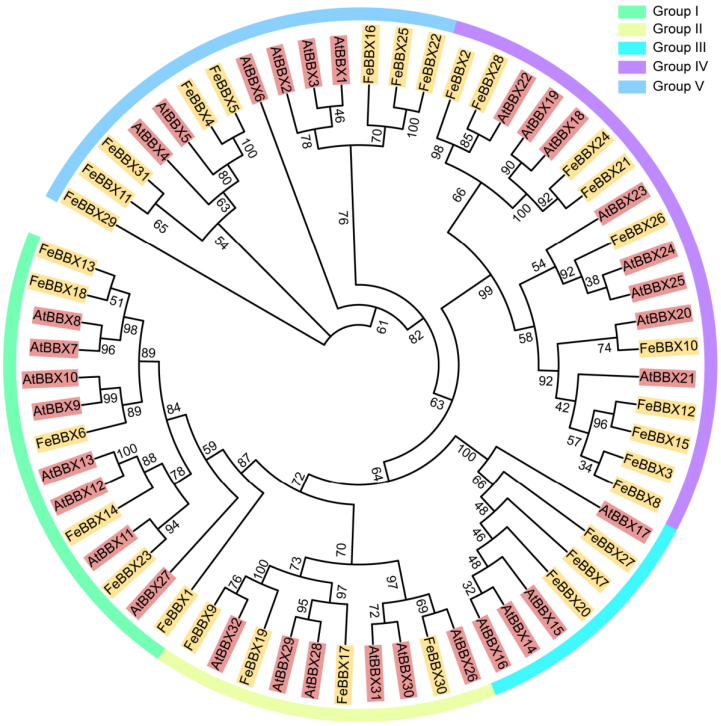


Figure 1. The phylogenetic tree of common buckwheat protein established according to *Arabidopsis thaliana*.

Chromosomal localization placed these genes on chromosomes Chr1 to Chr8 (Figure 2a). In addition, syntenic relationships were observed both among buckwheat chromosomes and between buckwheat and Arabidopsis chromosomes (Figure 2b). For example, FeBBX8 showed obvious synteny with AtBBX20 and AtBBX21, suggesting that some BBX genes have maintained conserved chromosomal blocks during the course of evolution.

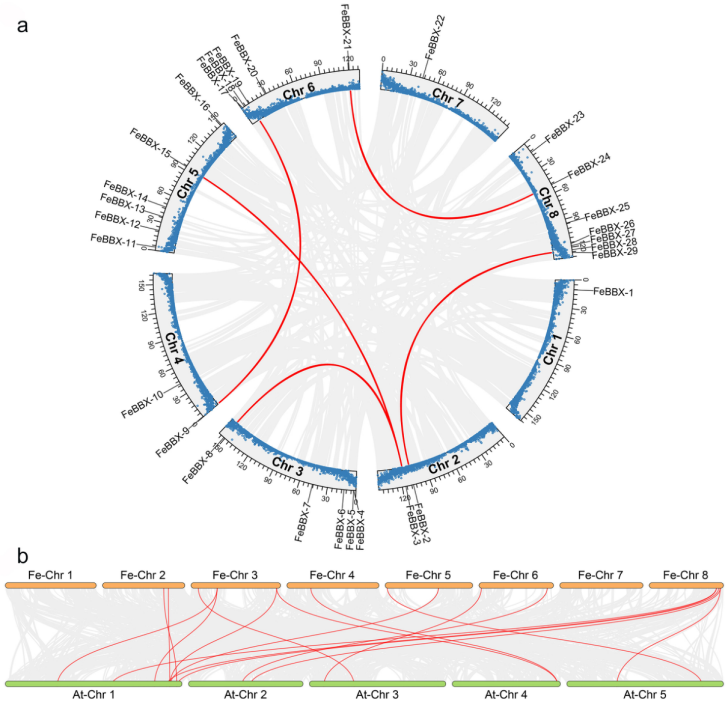


Figure 2. Chromosomal distribution and synteny analysis of FeBBX genes: (**a**) Chromosomal distribution and intra-genomic synteny of FeBBX genes in common buckwheat. (**b**) Inter-species synteny analysis between common buckwheat and *Arabidopsis thaliana*.

3.2. Gene Structure and Conserved Domains of FeBBXs

To elucidate the structural features of *FeBBX* genes, we compared their coding sequences against the corresponding genomic DNA sequences, thereby revealing the exon–intron organization (Figure 3a). *FeBBX9*, *FeBBX19*, and *FeBBX30* had no introns. Nine genes had one intron, eight genes had two introns, six genes had three introns, and five genes had five introns. We then predicted the conserved motifs of the 31 protein sequences (Figure 3b). In subgroup I (FeBBX1, FeBBX6, FeBBX13, FeBBX14, FeBBX18, and FeBBX23), all proteins contained two B-box domains and one CCT domain, except for FeBBX14. The members of subgroup II (FeBBX9, FeBBX17, FeBBX19, and FeBBX30) each had only one B-box domain. The members of subgroup III (FeBBX7, FeBBX20, and FeBBX27) each contained one B-box and one CCT domain. All members of subgroup IV, the largest subgroup, had two B-box domains but no CCT domain, except for FeBBX12. Subgroup V contained the most complex members.

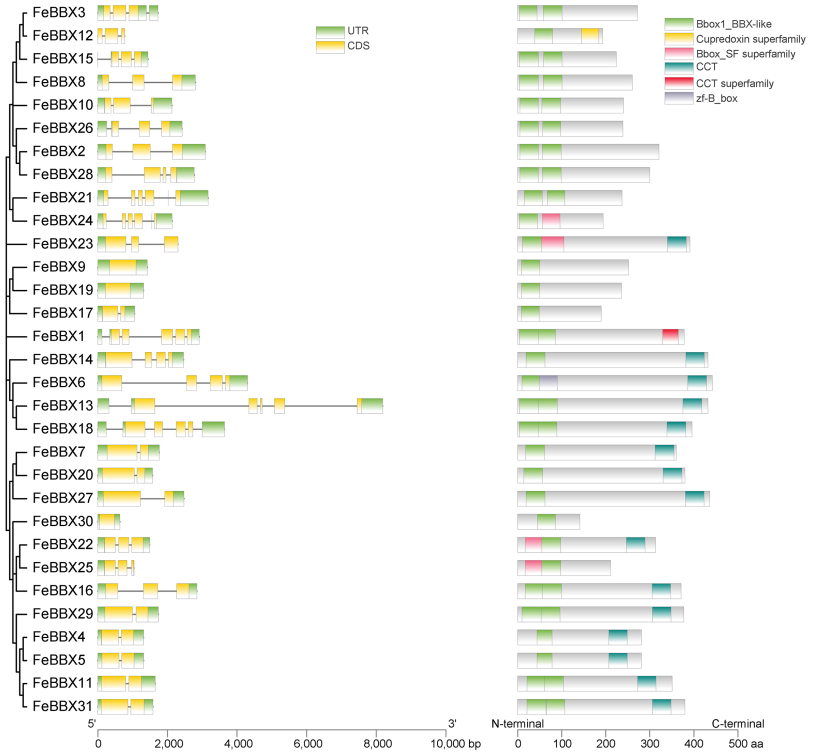


Figure 3. Molecular characterization of *FeBBXs*: (**a**) Gene structure of *FeBBX* genes. (**b**) B-box and CCT domains of FeBBX proteins.

3.3. Promoter Cis-Element Analysis of FeBBXs

The 2000 bp sequence upstream of the coding region was retrieved for each of the 31 *FeBBX* genes and submitted to PlantCARE for analysis. The promoters of the 31 genes contain various cis-elements, including light-responsive, hormone-responsive, and stress-responsive elements (Figure 4).

3.4. Expression Patterns of FeBBXs

Flavonoids in plants are mainly synthesized in glandular trichomes, which are widely distributed on leaves, stems, fruits, and roots. In order to investigate the tissue-specific expression of *FeBBX* genes in buckwheat, we established their transcript profiles across various tissues (Figure 5a). *FeBBX1*, *FeBBX6*, *FeBBX12*, *FeBBX16*, *FeBBX20*, *FeBBX22*, *FeBBX24*, *FeBBX25*, *FeBBX26*, *FeBBX27*, and *FeBBX29* were highly expressed in stems and leaves, while their expression in roots and fruits was relatively low. *FeBBX4*, *FeBBX5*,

FeBBX9, *FeBBX11*, and *FeBBX31* were highly expressed only in leaves. The expression of *FeBBX1*, *FeBBX4*, *FeBBX5*, *FeBBX9*, *FeBBX11*, *FeBBX16*, *FeBBX20*, *FeBBX22*, *FeBBX25*, *FeBBX26*, *FeBBX27*, *FeBBX29*, and *FeBBX31* showed an upward trend and reached its highest level in the leaves. We additionally examined the expression levels of FeBBX genes under different light intensities (Figure 5b). The expression of all *FeBBX* genes bar *FeBBX6*, *FeBBX12*, and *FeBBX30* was affected by light. The transcript levels of *FeBBX3*, *FeBBX8*, *FeBBX10*, *FeBBX13*, *FeBBX14*, *FeBBX15*, *FeBBX18*, and *FeBBX28* decreased as the light intensity weakened, while those of *FeBBX4*, *FeBBX5*, *FeBBX23*, *FeBBX26*, and *FeBBX27* rose as the light intensity increased.

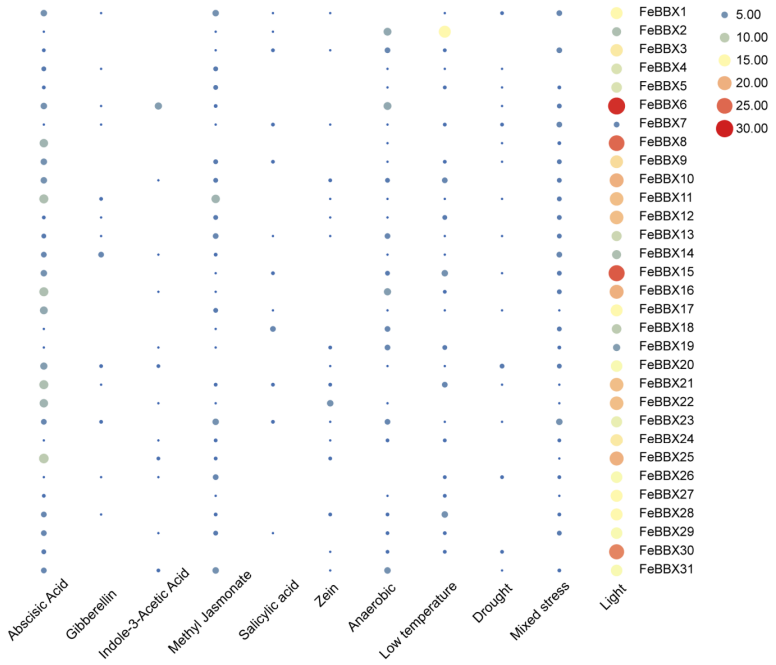


Figure 4. Cis-regulatory elements on the promoter regions of *FeBBX* genes.

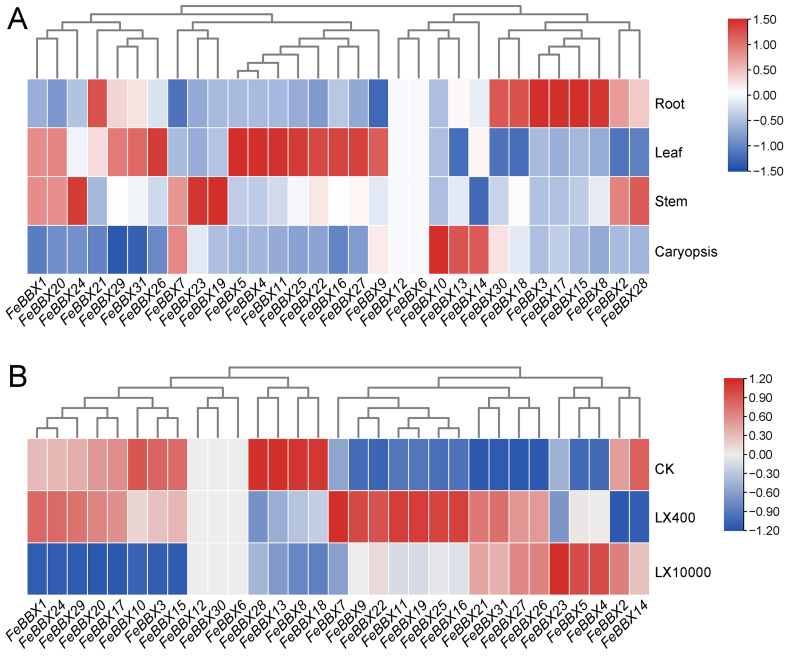


Figure 5. Expression profiling of *FeBBX* genes: (**a**) The expression level of *FeBBXs* in roots, leaves, stems and the caryopsis. (**b**) The expression level of *FeBBXs* at different light intensities.

3.5. Subcellular Localization of FeBBX11/27

To further investigate the role of FeBBX genes in flavonoid biosynthesis, we performed a phylogenetic analysis and found that FeBBX11 and FeBBX27 share high homology with previously reported flavonoid biosynthesis-related proteins (Figure S1), including AtBBX29 [44], IbBBX29 [31], PfBBX10 [45], PfBBX12 [45], and PfBBX17 [45]. Given their strong light responsiveness and high expression in leaves, FeBBX11 and FeBBX27 were selected as the top candidates for further functional analysis. We conducted subcellular localization assays on these two proteins. These genes were then cloned and ligated into the pHZM27g-GFP vector. Finally, green fluorescence signaling in the nucleus was observed under a confocal microscope (Figure 6).

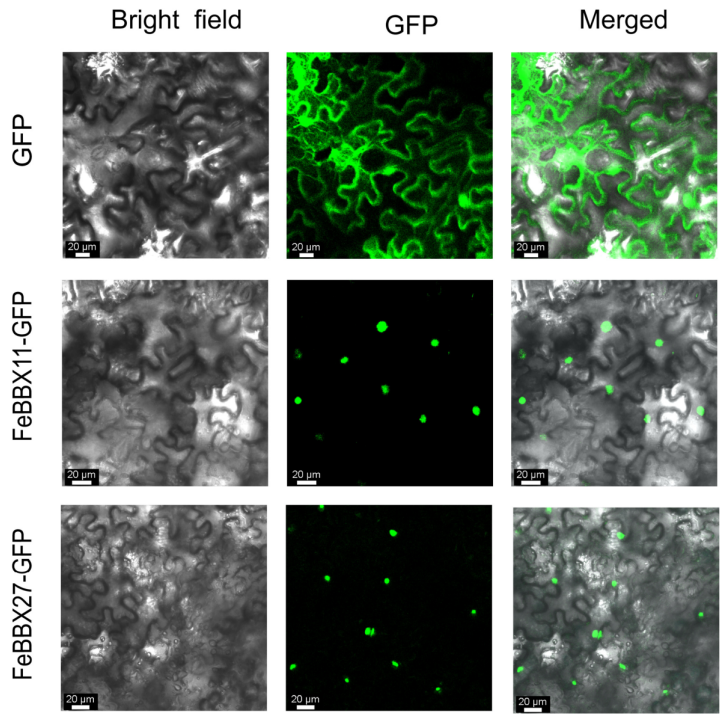


Figure 6. The green fluorescence signal of FeBBX11/27 proteins.

3.6. FeBBX11/27 Positively Regulates Flavonoid Biosynthesis

To further explore the transcriptional regulatory functions of FeBBX11 and FeBBX27 in the flavonoid biosynthesis pathway, we generated transgenic hairy roots with stable overexpression of *FeBBX11* and *FeBBX27* (Figure 7a–c) in common buckwheat, and we measured their secondary metabolite accumulation and antioxidant activity. The physiological and biochemical results showed that, compared with the empty-vector group, the total phenolic content in the *FeBBX11*-OE and *FeBBX27*-OE lines increased significantly to 131% and 172% (Figure 7d), and the total flavonoid content increased to 125% and 144% (Figure 7e), respectively. This indicates that the overexpression of these two transcription factors can markedly promote the accumulation of phenols and flavonoids in the phenylpropanoid pathway. Meanwhile, the antioxidant capacity assays revealed that both the ferric reducing antioxidant power (FRAP) and ABTS free radical scavenging activity at certain overexpression levels were significantly higher than those of the empty vector (Figure 7f,g). Specifically, *FeBBX27*-OE enhanced ABTS scavenging activity, suggesting a more targeted regulatory role on certain subgroups of flavonoids. Taken together, these results demonstrate that both *FeBBX11* and *FeBBX27* act as positive regulators of flavonoid biosynthesis, promoting the accumulation of antioxidant secondary metabolites, with FeBBX27 showing certain advantages in regulatory strength and functional breadth.

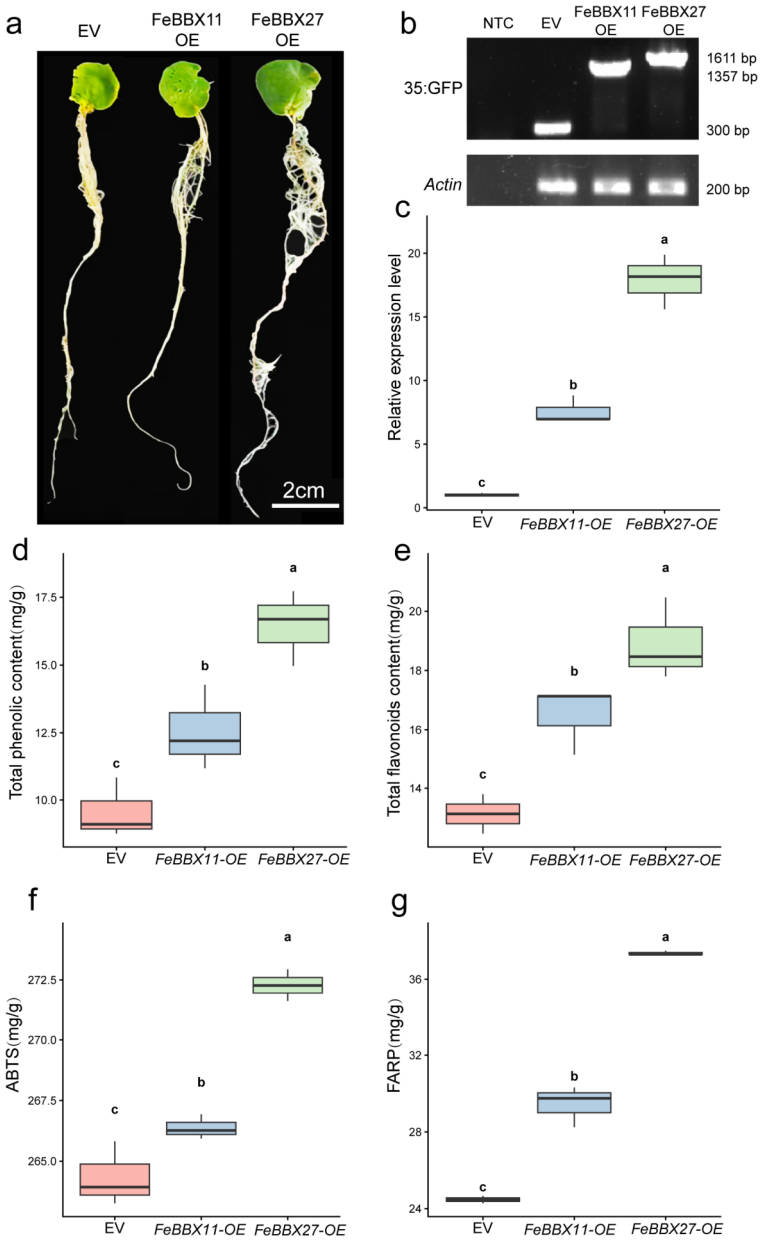


Figure 7. (**a**) Buckwheat tissue with stable overexpression of FeBBX11 and FeBBX27. (**b**) The positive detection of over-expressed hairy roots and agarose gel electrophoresis results of internal reference gene actin. (**c**) The gene expression level after overexpression of FeBBX11 and FeBBX27. (**d**) Total phenolic content in *FeBBX11/27*-overexpressing buckwheat roots compared with empty-vector tissue. (**e**) Total flavonoid content in *FeBBX11/27*-overexpressing buckwheat plants compared with EV. (**f**,**g**) The ferric reducing antioxidant power (FRAP) and ABTS free radical scavenging activity in *FeBBX11/27*-overexpressing roots compared with EV.

4. Discussion

Many studies have recently explored the functions of the BBX transcription factor family in secondary metabolism. However, the role of BBX proteins in flavonoid biosynthesis in buckwheat remains largely unknown. Previous studies identified 32 BBX members in Arabidopsis [46], 29 in tomato [47], 30 in rice [48], 96 in wheat [49], and 25 in pepper [50]. In this study, we identified 31 BBX genes in buckwheat. The variation in BBX family size among species suggests a history of species-specific expansion or contraction. Physicochemical analysis predicted that all 31 FeBBX proteins are hydrophilic and unstable (Table S1), consistent with the general characteristics of BBX proteins in other plants; this may reflect

their involvement in dynamic regulatory processes such as signal transduction [51]. Phylogenetic analysis revealed a close relationship of FeBBX proteins to Arabidopsis AtBBX proteins. Based on this conserved evolutionary relationship, preliminary functional predictions could be made for certain FeBBX genes. For instance, FeBBX8 clustered in the same clade as the light-responsive genes AtBBX20 and AtBBX21, suggesting a similar role in light-induced pigment accumulation in common buckwheat [52].

Gene structure analysis revealed that the 31 FeBBX genes contain relatively few introns. Such simple gene structures are often associated with rapid transcriptional responses under stress, representing an efficient regulatory strategy for environmental adaptation [53]. In conserved motif analysis, members within the same subfamily shared highly similar motif compositions, supporting the co-evolution of gene structure and function within this family [54]. Promoter analysis indicated an enrichment of FeBBX promoters in promoter elements linked to environmental stress adaptation and light signal transduction. Thus, FeBBX proteins may mediate crosstalk between light and stress signaling pathways, thereby contributing to stress adaptation. This is consistent with reports in other species. For example, the promoter of CmBBX20 in chrysanthemum contains light-responsive GATA and TCT motifs, and its expression is regulated by light signals [29]. In *Camellia sinensis*, the light-responsive transcription factor HY5 functions as a major regulator of light-induced anthocyanin metabolism [55]. In *Arabidopsis thaliana*, the transcription feedback loop consisting of AtBBX28, AtBBX29, AtBBX30, AtBBX31 and AtHY5 is responsible for fine regulation of morphogenesis in plants in response to light signals [56]. Therefore, the involvement of FeBBX genes in buckwheat flavonoid biosynthesis may also be subject to light regulation.

Functional divergence among BBX family members has been widely documented. In *Ipomoea batatas*, IbBBX24 enhances abiotic stress tolerance by forming complexes that scavenge ROS [57]. In *Glycine max*, the expression profiles of 59 GmBBX genes varied considerably under salt stress [58]. Similarly, tomato plants overexpressing SlBBX17 exhibited increased membrane stability, higher antioxidant enzyme activity, and reduced ROS accumulation under heat stress, leading to enhanced thermotolerance [59]. Considering the stress-induced expression patterns of FeBBX genes observed in this study, some FeBBX members may regulate antioxidant-related genes to maintain redox homeostasis and photosynthetic stability under stress. Subcellular localization positioned FeBBX11-GFP and FeBBX27-GFP fusion proteins in the nucleus (Figure 6), consistent with their predicted roles as transcription factors. In tissue-specific expression analysis, FeBBX11 and FeBBX27 were most highly expressed in leaf tissues (Figure 5), suggesting their potential involvement in responses to environmental stimuli [60]. To confirm their functions, we generated transgenic buckwheat hairy roots overexpressing FeBBX11 and FeBBX27. The total phenolic and total flavonoid contents in transgenic roots were 1.25- to 1.44-fold higher than in empty-vector controls, demonstrating FeBBX11 and FeBBX27's function as positive regulators of flavonoid biosynthesis in common buckwheat; they may also contribute to oxidative stress tolerance by mitigating ROS-induced damage. This study provides potential genetic evidence for the mechanisms by which the BBX family transcription factors regulate the flavonoid metabolic network in buckwheat; it also offers potential candidate genes for the molecular improvement of high-quality functional buckwheat germplasms.

5. Conclusions

We identified 31 FeBBX family members in the common buckwheat genome using bioinformatic approaches. They are unevenly distributed across eight chromosomes and encode unstable hydrophilic proteins that are predominantly localized in the nucleus. Phylogenetic analysis divided the FeBBX proteins into five subfamilies, with members of the

same subfamily sharing highly similar conserved motifs and domains. All FeBBX promoters contained conserved light- and abscisic acid-responsive elements, along with numerous cis-acting elements related to abiotic stress, hormones, and development. Expression analysis under different light treatments showed that many FeBBX genes respond to light signals. Among them, *FeBBX11* and *FeBBX27* were identified as core genes specifically associated with flavonoid biosynthesis, and they may participate in the stress-resistance regulatory network of common buckwheat. In summary, this study provides important candidate genes for understanding the molecular mechanisms of FeBBX-mediated stress tolerance and secondary metabolite accumulation.

Supplementary Materials: The following supporting information can be downloaded at https://www.mdpi.com/article/10.3390/agriculture16202183/s1. Table S1: Protein information of each BBX family member in common buckwheat. Table S2: Sequences of primers and probes used in this study. Figure S1: The relationship between light-induced members of BBX family and other flavonoid-related members reported in the literature. Table S3: The relationship between light-induced members of BBX family and other flavonoid-related members reported in the literature.

Author Contributions: Writing—original draft preparation, L.L.; writing—review and editing, L.L., Y.L., Z.H. and Z.F.; visualization, L.L., Y.L., Y.B., Z.L., Z.H. and Z.F.; supervision, Z.H. and Z.F.; project administration, Z.F.; funding acquisition, Z.F. All authors have read and agreed to the published version of the manuscript.

Funding: This work was supported by the Scientific Research Start-up Foundation for Advanced Talents of Yangtze University.

Institutional Review Board Statement: Not applicable.

Data Availability Statement: The data presented in this study are available on request from the corresponding author.

Conflicts of Interest: The authors declare no conflicts of interest.

Abbreviations

The following abbreviations are used in this manuscript:

C4L	4-Coumarate: CoA Ligase
UFGT	UDP-glucose: flavonoid 3-O-glucosyltransferase
C4H	Cinnamate 4-hydroxylase
MYB	Myeloblastosis
bHLH	Basic Helix–Loop–Helix
WD40	WD40 repeat-containing domain
NAC	NAM (No Apical Meristem) ATAF1/2 (Arabidopsis Transcription Activation Factor 1/2) CUC2 (CUP-SHAPED COTYLEDON 2)
BBX	B-box
FT	Flowering Locus T
CDS	Coding Sequence
GFP	Green Fluorescent Protein
HCl	Hydrochloric Acid
FRAP	Ferric Reducing Antioxidant Power
ABTS	2,2′-Azino-bis(3-ethylbenzothiazoline-6-sulfonate)

References

1. Xing, M.Y.; Cao, Y.L.; Grierson, D.; Sun, C.; Li, X. The chemistry, distribution, and metabolic modifications of fruit flavonols. *Fruit Res.* **2021**, *1*, 11. [CrossRef]
2. Chakraborty, S. Flavonoid: A Natural Scaffold with Modulatory Activities on Diverse Cellular Signaling Pathways Related to Complex Diseases. *Curr. Top. Med. Chem.* **2022**, *22*, 734. [CrossRef] [PubMed]

3. Singh, D.; Singh, N.; Dwivedi, S.; Trivedi, P.K. Transcriptional regulation of secondary plant product biosynthesis: Insights into flavonoid, alkaloid, and terpenoid pathways. *Plant Cell Tissue Organ Cult.* **2024**, *160*, 6. [CrossRef]
4. Liu, W.; Feng, Y.; Yu, S.; Fan, Z.; Li, X.; Li, J.; Yin, H. The Flavonoid Biosynthesis Network in Plants. *Int. J. Mol. Sci.* **2021**, *22*, 12824. [CrossRef] [PubMed]
5. Shen, N.; Wang, T.F.; Gan, Q.; Liu, S.; Wang, L.; Jin, B. Plant flavonoids: Classification, distribution, biosynthesis, and antioxidant activity. *Food Chem.* **2022**, *383*, 132531. [CrossRef] [PubMed]
6. Wang, D.; Bu, T.; Li, Y.Q.; He, Y.; Yang, F.; Zou, L. Pharmacological Activity, Pharmacokinetics, and Clinical Research Progress of Puerarin. *Antioxidants* **2022**, *11*, 2121. [CrossRef] [PubMed]
7. Lv, J.Y.; Shi, S.Q.; Zhang, B.X.; Xu, X.; Zheng, H.; Li, Y.; Cui, X.; Wu, H.; Song, Q. Role of puerarin in pathological cardiac remodeling: A review. *Pharmacol. Res.* **2022**, *178*, 106152. [CrossRef] [PubMed]
8. Naz, R.; Saqib, F.; Awadallah, S.; Wahid, M.; Latif, M.F.; Iqbal, I.; Mubarak, M.S. Food Polyphenols and Type II Diabetes Mellitus: Pharmacology and Mechanisms. *Molecules* **2023**, *28*, 3996. [CrossRef] [PubMed]
9. Yang, W.; Su, Y.; Dong, G.; Qian, G.; Shi, Y.; Mi, Y.; Zhang, Y.; Xue, J.; Du, W.; Shi, T.; et al. Liquid chromatography–mass spectrometry-based metabolomics analysis of flavonoids and anthraquinones in *Fagopyrum tataricum* L. Gaertn. (tartary buckwheat) seeds to trace morphological variations. *Food Chem.* **2020**, *331*, 127354. [CrossRef] [PubMed]
10. Kreft, S.; Knapp, M.; Kreft, I. Extraction of Rutin from Buckwheat (*Fagopyrum esculentum* Moench) Seeds and Determination by Capillary Electrophoresis. *J. Agric. Food Chem.* **1999**, *47*, 4649–4652. [CrossRef] [PubMed]
11. Ke, J.; Ran, B.; Sun, P.; Cheng, Y.; Chen, Q.; Li, H. An Evaluation of the Absolute Content of Flavonoids and the Identification of Their Relationship with the Flavonoid Biosynthesis Genes in Tartary Buckwheat Seeds. *Agronomy* **2023**, *13*, 3006. [CrossRef]
12. Kim, J.; Kim, R.H.; Hwang, K.T. Flavonoids in different parts of common buckwheat (*Fagopyrum esculentum*) and Tartary buckwheat (*F. tataricum*) during growth. *J. Food Compos. Anal.* **2023**, *120*, 105362. [CrossRef]
13. He, Q.; Ma, D.; Li, W.; Xing, L.; Zhang, H.; Wang, Y.; Du, C.; Li, X.; Jia, Z.; Li, X.; et al. High-quality *Fagopyrum esculentum* genome provides insights into the flavonoid accumulation among different tissues and self-incompatibility. *J. Integr. Plant Biol.* **2023**, *65*, 1423–1441. [CrossRef] [PubMed]
14. Jiang, L.; Gao, Y.; Han, L.; Zhang, W.; Fan, P. Designing plant flavonoids: Harnessing transcriptional regulation and enzyme variation to enhance yield and diversity. *Front. Plant Sci.* **2023**, *14*, 1220062. [CrossRef] [PubMed]
15. Huang, J.; Zhao, X.; Zhang, Y.; Chen, Y.; Zhang, X.; Yi, Y.; Ju, Z.; Sun, W. Chalcone-Synthase-Encoding RdCHS1 Is Involved in Flavonoid Biosynthesis in *Rhododendron delavayi*. *Molecules* **2024**, *29*, 1822. [CrossRef] [PubMed]
16. Jayaraman, K.; Raman, V.K.; Sevanthi, A.M.; Sivakumar, S.R.; Gayatri, T.; Viswanathan, C.; Mohapatra, T.; Mandal, P.K. Stress-inducible expression of chalcone isomerase2 gene improves accumulation of flavonoids and imparts enhanced abiotic stress tolerance to rice. *Environ. Exp. Bot.* **2021**, *190*, 104582. [CrossRef]
17. Yin, T.; Xu, R.; Zhu, L.; Yang, X.; Zhang, M.; Li, X.; Zi, Y.; Wen, K.; Zhao, K.; Cai, H.; et al. Comparative analysis of the PAL gene family in nine citruses provides new insights into the stress resistance mechanism of Citrus species. *BMC Genom.* **2024**, *25*, 1020. [CrossRef] [PubMed]
18. Xu, W.J.; Dubos, C.; Lepiniec, L. Transcriptional control of flavonoid biosynthesis by MYB–bHLH–WDR complexes. *Trends Plant Sci.* **2015**, *20*, 176–185. [CrossRef] [PubMed]
19. Fang, H.; Wan, Y.; Liu, H.; Qi, X.; Yu, X.; Chen, Z.; Liu, Q.; Li, L.; Bai, Y.; Liu, D.; et al. Characterization of the *Lonicera japonica* R2R3-MYB transcription factor gene LjaMYB305 that promotes the flavonoid biosynthesis. *Plant Sci.* **2025**, *359*, 112654. [CrossRef] [PubMed]
20. Huang, X.; He, Y.; Zhang, K.; Shi, Y.; Zhao, H.; Lai, D.; Lin, H.; Wang, X.; Yang, Z.; Xiao, Y.; et al. Evolution and Domestication of a Novel Biosynthetic Gene Cluster Contributing to the Flavonoid Metabolism and High-Altitude Adaptability of Plants in the Fagopyrum Genus. *Adv. Sci.* **2024**, *11*, 2403603. [CrossRef] [PubMed]
21. Li, C.; Yang, J.; Yang, K.; Wu, H.; Chen, H.; Wu, Q.; Zhao, H. Tartary buckwheat FtF3′H1 as a metabolic branch switch to increase anthocyanin content in transgenic plant. *Front. Plant Sci.* **2022**, *13*, 959698. [CrossRef] [PubMed]
22. Wang, D.; Yang, T.; Li, Y.; Deng, F.; Dong, S.; Li, W.; He, Y.; Zhang, J.; Zou, L. Light Intensity—A Key Factor Affecting Flavonoid Content and Expression of Key Enzyme Genes of Flavonoid Synthesis in Tartary Buckwheat. *Plants* **2022**, *11*, 2165. [CrossRef] [PubMed]
23. Wang, J.; Li, W.; Fan, D.; He, Y.; Shi, Y.; Lin, H.; Fauconnier, M.; Purcaro, G.; Quinet, M.; Genva, M.; et al. Natural Variation in the FtNAC2 Promoter Regulates Quercetin Accumulation and Drought Tolerance in Tartary Buckwheat. *Plant Cell Environ.* **2026**, *49*, 1382–1398. [CrossRef] [PubMed]
24. Ren, S.; Cui, J.; Wang, L.; Lu, Z.; Jin, B. Plant Flavonoids: Biosynthesis, Regulation, and Roles in Biotic and Abiotic Stresses. *Plant Cell Environ.* **2026**, *49*, 5664–5684. [CrossRef] [PubMed]
25. Nam, T.G.; Kim, D.O.; Eom, S.H. Effects of light sources on major flavonoids and antioxidant activity in common buckwheat sprouts. *Food Sci. Biotechnol.* **2018**, *27*, 169–176. [CrossRef] [PubMed]

26. Tian, X.; Hu, M.; Yang, J.; Yin, Y.; Fang, W. Ultraviolet-B Radiation Stimulates Flavonoid Biosynthesis and Antioxidant Systems in Buckwheat Sprouts. *Foods* **2024**, *13*, 3650. [CrossRef] [PubMed]
27. Luo, Z.; Tu, L.; Luo, Y.; Wang, Y.; Wang, L.; Yan, F. Precise scheduling of B-box transcription factors: The core network for balancing plant growth, metabolism and stress resistance. *Front. Plant Sci.* **2026**, *17*, 1809754. [CrossRef] [PubMed]
28. Putterill, J.; Robson, F.; Lee, K.; Simon, R.; Coupland, G. The CONSTANS gene of Arabidopsis promotes flowering and encodes a protein showing similarities to zinc finger transcription factors. *Cell* **1995**, *80*, 847–857. [CrossRef] [PubMed]
29. Li, J.; Li, S.; Hua, Z.; Hao, J.; Wang, P.; Zhu, M.; Zhang, J.; Liu, S.; Li, D.; Liu, Y.; et al. Genome-wide characterization of B-box gene family in eggplant and functional identification of SmBBX22 in modulating anthocyanin synthesis. *Hortic. Plant J.* **2026**, *12*, 670–689. [CrossRef]
30. Li, C.; Pei, J.; Yan, X.; Cui, X.; Tsuruta, M.; Liu, Y.; Lian, C. A poplar B-box protein PtrBBX23 modulates the accumulation of anthocyanins and proanthocyanidins in response to high light. *Plant Cell Environ.* **2021**, *44*, 3015–3033. [CrossRef] [PubMed]
31. Gao, X.R.; Zhang, H.; Li, X.; Bai, Y.-W.; Peng, K.; Wang, Z.; Dai, Z.-R.; Bian, X.-F.; Zhang, Q.; Jia, L.-C.; et al. The B-box transcription factor IbBBX29 regulates leaf development and flavonoid biosynthesis in sweet potato. *Plant Physiol.* **2023**, *191*, 496–514. [CrossRef] [PubMed]
32. Iqbal, M.; Zhang, L.; Yin, Y.; Yang, Z.; Zhang, J.; Wang, L. MdBBX47, a B-box transcription factor directly and indirectly regulates ALA-induced anthocyanin accumulation in apple. *BMC Plant Biol.* **2026**, *26*, 1038. [CrossRef] [PubMed]
33. Liu, X.; Sun, W.; Ma, B.; Song, Y.; Guo, Q.; Zhou, L.; Wu, K.; Zhang, X.; Zhang, C. Genome-wide analysis of blueberry B-box family genes and identification of members activated by abiotic stress. *BMC Genom.* **2023**, *24*, 584. [CrossRef] [PubMed]
34. Wang, J.; Meng, Z.; He, H.; Du, P.; Dijkwel, P.P.; Shi, S.; Li, H.; Xie, Q. Genome-Wide Analysis of BBX Gene Family in Three Medicago Species Provides Insights into Expression Patterns Under Hormonal and Salt Stresses. *Int. J. Mol. Sci.* **2024**, *25*, 5778. [CrossRef] [PubMed]
35. Feng, J.; Chen, C.; Wu, Y.; Fan, L.; Zhang, Z.; Chen, M.; Tang, H.; Yu, G.; Ren, J.; Luo, J.; et al. How to make big data accessible to plant biologists and beyond: Ten years of lessons from TBtools. *Mol. Plant* **2026**, *19*, 1378–1391. [CrossRef] [PubMed]
36. Mello, B. Estimating TimeTrees with MEGA and the TimeTree Resource. *Mol. Biol. Evol.* **2018**, *35*, 2334–2342. [CrossRef] [PubMed]
37. Chen, C.; Wu, Y.; Li, J.; Wang, X.; Zeng, Z.; Xu, J.; Liu, Y.; Feng, J.; Chen, H.; He, Y.; et al. TBtools-II: A "one for all, all for one" bioinformatics platform for biological big-data mining. *Mol. Plant* **2023**, *16*, 1733–1742. [CrossRef] [PubMed]
38. Li, J.; Dong, Y.; Li, C.; Pan, Y.; Yu, J. SiASR4, the Target Gene of SiARDP from *Setaria italica*, Improves Abiotic Stress Adaption in Plants. *Front. Plant Sci.* **2017**, *7*, 2053. [CrossRef] [PubMed]
39. Zhang, K.; He, Y.; Lu, X.; Shi, Y.; Zhao, H.; Li, X.; Li, J.; Liu, Y.; Ouyang, Y.; Tang, Y.; et al. Comparative and population genomics of buckwheat species reveal key determinants of flavor and fertility. *Mol. Plant* **2023**, *16*, 1427–1444. [CrossRef] [PubMed]
40. Singleton, L.V.; Orthofer, R.; Lamuela-Raventós, M.R. Analysis of total phenols and other oxidation substrates and antioxidants by means of folin-ciocalteu reagent. *Methods Enzymol.* **1999**, *299*, 152–178. [CrossRef]
41. Zhishen, J.; Mengcheng, T.; Jianming, W. The determination of flavonoid contents in mulberry and their scavenging effects on superoxide radicals. *Food Chem.* **1999**, *64*, 555–559. [CrossRef]
42. Benzie, I.F.; Strain, J.J. The ferric reducing ability of plasma (FRAP) as a measure of "antioxidant power": The FRAP assay. *Anal. Biochem.* **1996**, *239*, 70–76. [CrossRef] [PubMed]
43. Re, R.; Pellegrini, N.; Proteggente, A.; Pannala, A.; Yang, M.; Rice-Evans, C. Antioxidant activity applying an improved ABTS radical cation decolorization assay. *Free Radic. Biol. Med.* **1999**, *26*, 1231–1237. [CrossRef] [PubMed]
44. Medina-Fraga, A.L.; Chinen, L.A.; Demkura, P.V.; Lichy, M.Z.; Gershenzon, J.; Ballaré, C.L.; Crocco, C.D. AtBBX29 integrates photomorphogenesis and defense responses in Arabidopsis. *Photochem. Photobiol. Sci.* **2023**, *22*, 1475–1489. [CrossRef] [PubMed]
45. Fei, C.; He, Y.; Chen, P.; Zhao, W.; Chen, B.; Qian, K.; Zhou, P. Genome-wide analysis of PfBBXs transcription factors in *Perilla frutescens* and their expression responses to different light intensities. *Plant Mol. Biol.* **2025**, *115*, 130. [CrossRef] [PubMed]
46. Khanna, R.; Kronmiller, B.; Maszle, D.R.; Coupland, G.; Holm, M.; Mizuno, T.; Wu, S.-H. The Arabidopsis B-Box Zinc Finger Family. *Plant Cell* **2009**, *21*, 3416–3420. [CrossRef] [PubMed]
47. Chu, Z.; Wang, X.; Li, Y.; Yu, H.; Li, J.; Lu, Y.; Li, H.; Ouyang, B. Genomic Organization, Phylogenetic and Expression Analysis of the B-BOX Gene Family in Tomato. *Front. Plant Sci.* **2016**, *7*, 1552. [CrossRef] [PubMed]
48. Huang, J.; Zhao, X.; Weng, X.; Wang, L.; Xie, W. The Rice B-Box Zinc Finger Gene Family: Genomic Identification, Characterization, Expression Profiling and Diurnal Analysis. *PLoS ONE* **2012**, *7*, e48242. [CrossRef] [PubMed]
49. Cheng, X.; Lei, S.; Li, J.; Tian, B.; Li, C.; Cao, J.; Lu, J.; Ma, C.; Chang, C.; Zhang, H. In silico analysis of the wheat BBX gene family and identification of candidate genes for seed dormancy and germination. *BMC Plant Biol.* **2024**, *24*, 334. [CrossRef] [PubMed]
50. Yong, Z.; Yu, L.; Ting, Y.; Li, J.; Qiu, X.; Zhu, C.; Liu, J.; Dang, F.; Yang, Y. Characterization of the B-BOX gene family in pepper and the role of CaBBX14 in defense response against *Phytophthora capsici* infection. *Int. J. Biol. Macromol.* **2023**, *237*, 124071. [CrossRef] [PubMed]
51. Talar, U.; Kiełbowicz-Matuk, A. Beyond Arabidopsis: BBX Regulators in Crop Plants. *Int. J. Mol. Sci.* **2021**, *22*, 2906. [CrossRef] [PubMed]

52. Song, Z.; Bian, Y.; Liu, J.; Sun, Y.; Xu, D. B-box proteins: Pivotal players in light-mediated development in plants. *J. Integr. Plant Biol.* **2020**, *62*, 1293–1309. [CrossRef] [PubMed]
53. Ni, Y.; Guo, C.; Zhang, X.; Ma, M.; Liu, X.; Li, Y.; Lian, S.; Li, J.; Jiang, Y.; Niu, J.; et al. Evolutionary and functional diversification of the DOG gene family in wheat (*Triticum aestivum* L.) and their roles in seed dormancy. *BMC Genom.* **2025**, *26*, 861. [CrossRef] [PubMed]
54. Muhammad, I.; Jing, X.-Q.; Shalmani, A.; Ali, M.; Yi, S.; Gan, P.-F.; Li, W.-Q.; Liu, W.-T.; Chen, K.-M. Comparative In Silico Analysis of Ferric Reduction Oxidase (FRO) Genes Expression Patterns in Response to Abiotic Stresses, Metal and Hormone Applications. *Molecules* **2018**, *23*, 1163. [CrossRef] [PubMed]
55. Du, Y.; Zhang, H.; Rothenberg, D.O.N.; Jin, K.; Li, J.; Zhang, C.; Liao, W.; Cui, Y.; Chen, W.; Li, M.; et al. Molecular mechanism of light-responsive transcription factor ELONGATED HYPOCOTYL 5 regulating anthocyanin synthesis in tea (*Camellia sinensis*). *Int. J. Biol. Macromol.* **2025**, *339*, 149899. [CrossRef] [PubMed]
56. Song, Z.Q.; Yan, T.T.; Liu, J.J.; Bian, Y.; Heng, Y.; Lin, F.; Jiang, Y.; Deng, X.W.; Xu, D. BBX28/BBX29, HY5 and BBX30/31 form a feedback loop to fine-tune photomorphogenic development. *Plant J.* **2020**, *104*, 377–390. [CrossRef] [PubMed]
57. Zhang, H.; Wang, Z.; Li, X.; Gao, X.; Dai, Z.; Cui, Y.; Zhi, Y.; Liu, Q.; Zhai, H.; Gao, S.; et al. The IbBBX24–IbTOE3–IbPRX17 module enhances abiotic stress tolerance by scavenging reactive oxygen species in sweet potato. *New Phytol.* **2022**, *233*, 1133–1152. [CrossRef] [PubMed]
58. Shan, B.; Bao, G.; Shi, T.; Zhai, L.; Bian, S.; Li, X. Genome-wide identification of BBX gene family and their expression patterns under salt stress in soybean. *BMC Genom.* **2022**, *23*, 820. [CrossRef] [PubMed]
59. Xu, X.; Wang, Q.; Li, W.Q.; Hu, T.; Wang, Q.; Yin, Y.; Liu, X.; He, S.; Zhang, M.; Liang, Y.; et al. Overexpression of SlBBX17 affects plant growth and enhances heat tolerance in tomato. *Int. J. Biol. Macromol.* **2022**, *206*, 799–811. [CrossRef] [PubMed]
60. Yang, H.; Liu, J.; Ma, M.; Tan, Z.; Zhang, K.; Sun, R.; Zhan, X.; Cui, D. Leaf development and its interaction with phyllospheric microorganisms: Impacts on plant stress responses. *Plant Stress* **2025**, *16*, 100843. [CrossRef]

Disclaimer/Publisher's Note: The statements, opinions and data contained in all publications are solely those of the individual author(s) and contributor(s) and not of MDPI and/or the editor(s). MDPI and/or the editor(s) disclaim responsibility for any injury to people or property resulting from any ideas, methods, instructions or products referred to in the content.